GEOPHYSICAL RESEARCH LETTERS, VOL. 28, NO. 2, PAGES 363-366, JANUARY 15, 2001

Rupture History of September 30, 1999 Intraplate Earthquake of Oaxaca, Mexico (M_W=7.5) from Inversion of Strong-Motion Data

B. Hernandez,[1,3] N. M. Shapiro,[2] S. K. Singh,[2,4] J. F. Pacheco,[2] F. Cotton,[1]
M. Campillo,[3] A. Iglesias,[2] V. Cruz,[2] J. M. Gómez,[2] L. Alcántara[4]

Abstract. Near-source strong motions are inverted to estimate the rupture history of intraslab, normal-faulting September 30, 1999, Oaxaca, Mexico earthquake. Two focal mechanisms (Harvard and NEIC CMT solutions) are tested for the source geometry. The inversion with the NE dipping fault plane of the Harvard solution best matches the data (strike= 295°, dip= 50°, rake= −82°). We estimated the slip distribution on the fault and the associated rupture front propagation, as well as the rise time. The inversion results show that the rupture mainly propagated from ESE to WNW and slightly downdip, with an average rupture velocity of about 3 km/s. The rise time ranges between 1 and 2 s. The slip distribution on the fault is mainly concentrated in two interconnected patches with a maximum slip of 2.5 m located about 20 km and 40 km WNW of the hypocenter. Most of the slip is released at an average depth of 45 km. A smaller area with a maximum slip of 1.5 m is also observed close to the hypocenter. The total co-seismic moment released is equal to 1.8×10^{20} Nm.

Introduction

Until recently it was thought that large, normal-faulting earthquakes in the subducted Cocos plate, below Mexico, occurred downdip from the strongly-coupled part of the plate interface, at distances greater than about 150 km from the coast. An exception seemed to be the 15 January, 1931 (M=7.8) Oaxaca earthquake, which was located only about 65 km from the coast [*Singh et al.,* 1985]. Recent earthquakes, however, suggest that intraslab earthquakes, which occur below or near the downdip edge of coupled plate interface, may be more frequent than previously thought. For example, the earthquake of 10 December, 1994 (Mw=6.6) was located below the downdip edge of the rupture area of the 19 and 21 September, 1985 (Mw= 8.0, 7.6) Michoacan earthquakes [*Cocco et al.,* 1997] and the earthquake of 11 January, 1997 (Mw=7.3) occurred just below the 1985 rupture area [*Mikumo et al.,* 1999, 2000].

The two large earthquakes which occurred in Mexico during 1999 were both normal-faulting events: the 15 June 1999 (M_W=7.0) Tehuacán earthquake and 30 September 1999 (M_W=7.5), Oaxaca earthquake. Although both were intraplate events, there is a significant difference in their location. The Tehuacán earthquake was located about 200 km from the coast [*Singh et al.,* 1999]. The Oaxaca earthquake, on the other hand, occurred below the coast [*Singh et al.,* 2000], near the downdip edge of the aftershock area of the 29 November, 1978 (Mw=7.7) thrust earthquake [*Singh et al.,* 1980].

Detailed studies of the source process of intraplate earthquakes are important to understand the state of stress in the Cocos plate, the dynamics of its subduction, the stress interaction between interplate thrust- and intraplate normal-faulting earthquakes, and the seismic hazard in the region. The 1999 Oaxaca earthquake is the first large intraslab event in the subducted Cocos plate to be azimuthally well-recorded by eight near-source strong-motion stations. In this paper we perform inversion of these near-source records to constrain the rupture history of the earthquake.

Data

Figure 1 shows the eight strong-motion stations which were located within an epicentral distance of 150 km. The accelerographs are 18-bit Etna (sampling rate 200 Hz, range 2g). All stations were equipped with GPS receivers and recorded three components of the ground acceleration. The azimuthal coverage of the stations is reasonably good. The accelerograms were first doubly integrated to obtain the particle displacements. The traces were then filtered between 0.05 and 0.4 Hz, the frequency band used in our inversions. At lower frequencies the data are not reliable. At higher frequencies the structure is probably too complex to be adequately represented by a horizontally-layered half space, the model we use to generate synthetic seismograms.

Modelling

We assume the faulting to be confined to a single plane. Here we present the results based on the fo-

[1]IPSN, Fontenay-aux-Roses, France
[2]Instituto de Geofísica, UNAM, México
[3]LGIT, Université Joseph Fourier, Grenoble, France
[4]Instituto de Ingeniería, UNAM, México

Paper number 2000GL011975.
0094-8276/01/2000GL011975$05.00

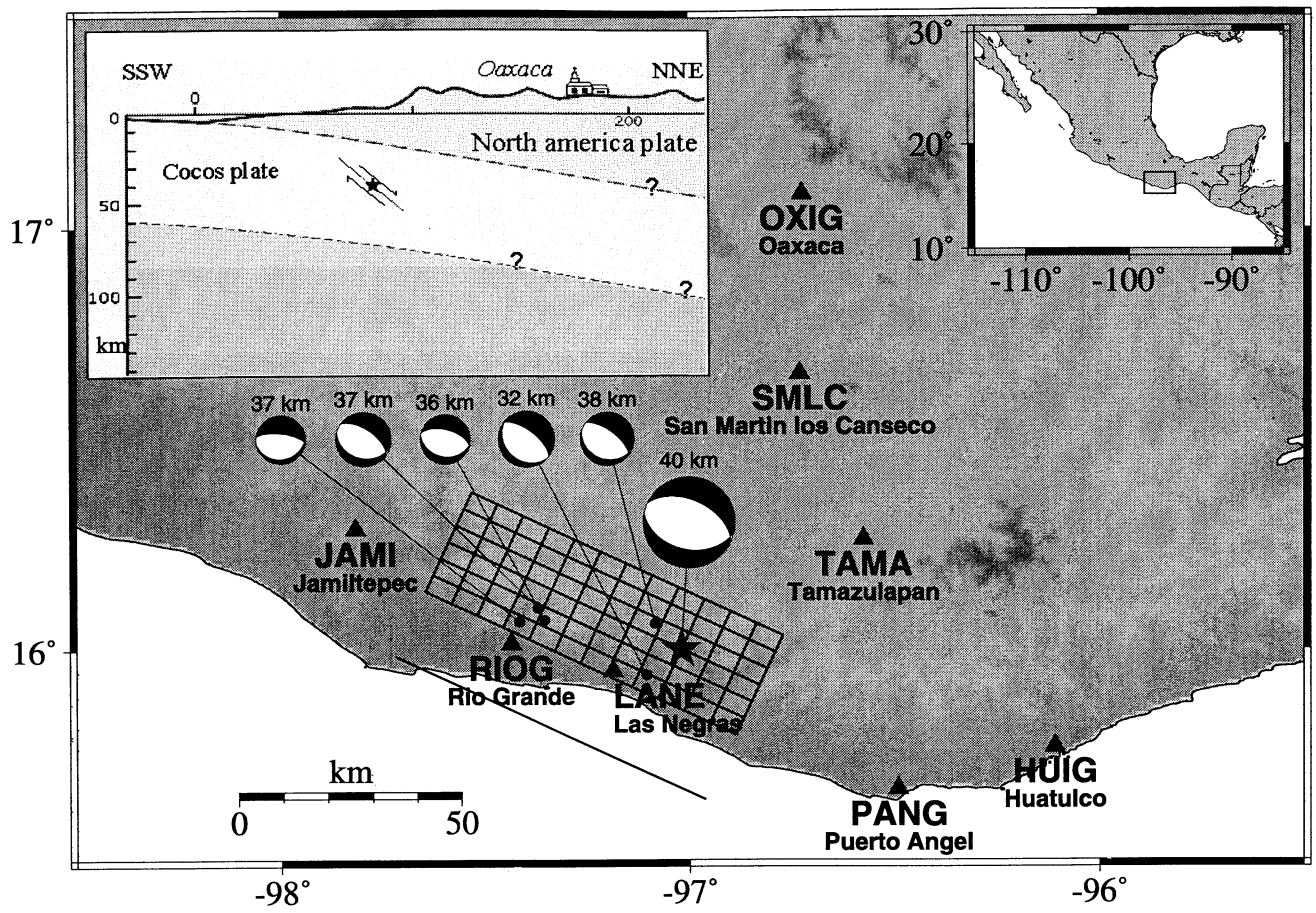

Figure 1. Location map showing the horizontal projection of the fault plane (divided into 72 square subfaults) and the eight strong-motion stations (triangles) used in this study. This model corresponds to the geometry of the Harvard CMT solution (strike= 295°, dip= 50°). Star shows the hypocenter location of the mainshock. The epicenter location, focal mechanism and depth of the early larger aftershock are also displayed on the map. A small map of Mexico with the location of the earthquake is shown in the top right corner, a cross-section of the subduction zone in the direction perpendicular to the azimuth of the fault is shown in the top left corner.

cal mechanism given in the Harvard CMT solution. Of the two nodal planes, we choose the one which dips NE (strike= 295°, dip= 50°, rake= −82°) as the fault plane. Inversions with the same parameterization but with the NEIC CMT solution (strike= 315°, dip= 55°, rake= −81°) lead to similar results but with a worse fit. The results obtained by choosing the second nodal plane of Harvard CMT solution as the fault plane also lead to a worse fit. The selection of NE-dipping nodal plane as the fault plane is also supported by five of the larger aftershocks [*Singh et al.*, 2000] which were located shallower and closer to the coast than the mainshock hypocenter (Figure 1). The fault model adopted is a rectangle with 90 km along the strike and 45 km along the dip. A visual inspection of local and regional data shows that the rupture propagated toward the WNW [*Singh et al.*, 2000]. For this reason, the fault length toward WNW of the hypocenter is taken to be greater than toward ESE. The hypocenter location (16.00°N, −97.02°E, H=39.7 km), obtained from local and regional data, is situated in the middle of the fault along the width and 22.5 km WNW to the SSE tip of the fault. We use a nonlinear least-square inversion scheme based on the work of *Tarantola and Valette* [1982] and discussed in detail by *Cotton and Campillo* [1995] and *Hernandez et al.* [1999]. We minimize the difference between observed and synthetic spectra (real and imaginary parts) for all the discrete frequencies between 0.05 and 0.4 Hz and for the three components of the eight stations. The fault is divided into 7.5 km x 7.5 km subfaults (Figure 1). Each subfault is composed of 64 source points whose rupture is delayed in time by assuming a constant 2.7 km/s rupture velocity inside the subfault. The velocity model used is shown in Table 1.

Inversion Results

We start with an homogeneous initial model. A constant 2 s rise time and a 1.3 m slip in the rake direction is assigned to each subfault. The initial rupture time of each subfault is computed with a 2.7 km/s rupture velocity. The fit between the data and the synthetics is

Table 1. Velocity model used for the Green's function calculation

H, m	$V_P, m.s^{-1}$	$V_S, m.s^{-1}$	$\rho, kg.m^{-3}$	Q_P	Q_S
0.	4500.	2600.	2700.	300.	100.
1000.	5300.	3060.	2700.	300.	100.
5000.	6200.	3580.	2700.	300.	100.
15000	6850.	3950.	2900.	300.	100.
30000.	8150.	4710.	3200.	300.	100.

improved iteratively perturbating the values of the rupture time, the rise time, and the slip amplitude which define the shape and the timing of the source function of each subfault. The perturbation of one parameter of the model from one iteration to the next depends not only on its initial value but also on its relative covariance. We assumed the same variance for the slip amplitude and the rise time of all the subfauts (variance=100.0). For the rupture time associated to each subfault we assumed a larger a priori variance (169.0). This means that the rupture velocity is allowed to vary significantly

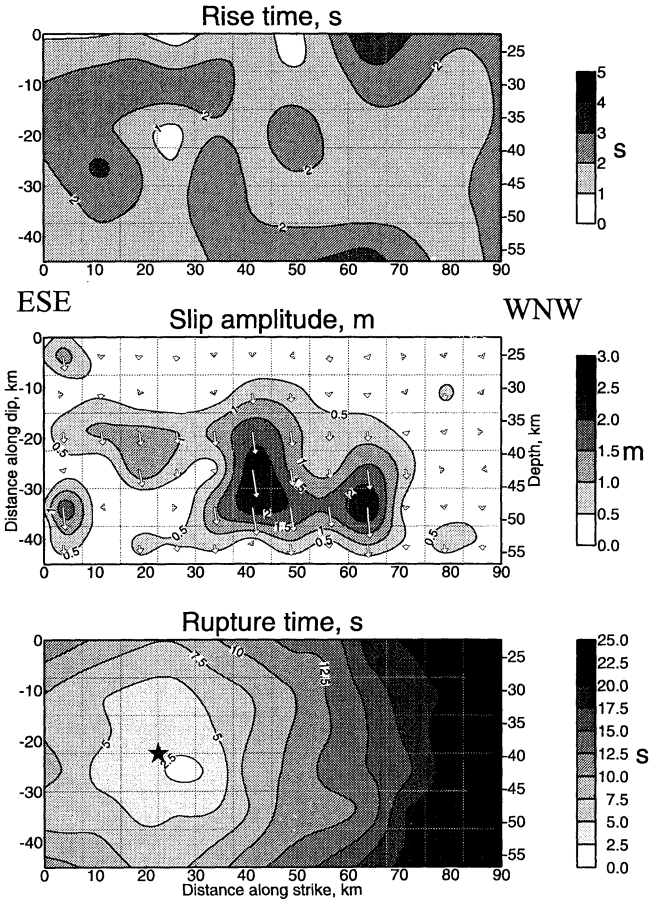

Figure 2. Maps of rise time, slip, and rupture time obtained by interpolation of the results of nonlinear inversion obtained for the fault geometry corresponding to the Harvard CMT solution. The arrows indicate the relative motion of the hanging wall. The star indicates the location of the hypocenter location of the initial model.

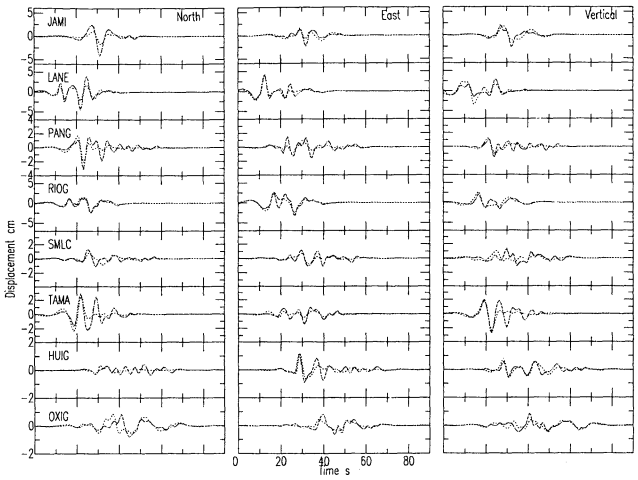

Figure 3. Strong-motion seismograms (solid lines) and synthetic seismograms (dotted lines). Synthetics and observations are plotted on the same scale. The synthetics correspond to the solution shown in Figure 2.

from its initial value. A small component perpendicular to the rake angle is allowed for the slip (variance=1.0) starting from an initial value of 0. m. We also need to define a covariance for the data which reflects their relative reliability. We gave the same weight to all the data (variance=1.0). This is reasonable because the stations are well distributed in space and the data are reliable in the frequency range considered. The data at all stations also appear to be free from significant site effects. The damping factor of the iterative inversion scheme is taken equal to 0.05.

The results of our inversion (Figure 2) show that the rupture mainly propagated from ESE to WNW and slightly downdip, with an average rupture velocity close to 3 km/s. The rise time (local duration of the rupture) range between 1 and 2 s. The slip distribution on the fault shows two areas of 2.5 m peak slip located about 20 km and 40 km WNW of the hypocenter at an average depth of 45 km. These two slip area are interconnected (Figure 2). A small area with a 2 m peak slip is observed close to the hypocenter. The synthetic seismograms calculated with the source model, described in Figure 2, are compared with the data in Figure 3. The match between synthetics and observation is about as good as can reasonably be expected (variance reduction = 48%), given the uncertainties in the velocity model. The source time function and the cumulated coseismic moment released as a function of time, corresponding to the kinematic model presented in Figure 2, is shown in Figure 4. We note that the total moment is about 1.8×10^{20} Nm, in agreement with the other estimates.

Conclusion

The September 30, 1999 Oaxaca earthquake was a normal-faulting event which occurred at a depth of about 45 km in the subducted Cocos plate. Our source image, based on the low-frequency content of strong-

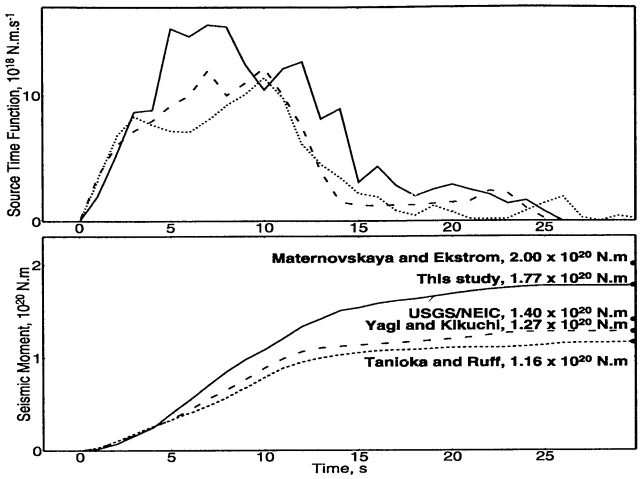

Figure 4. Source time function and cumulated moment corresponding to the model shown in Figure 2. The results are compared with other results based on teleseismic data.

motion data, shows that the rupture propagated from ESE to WNW and slightly downdip. A seismic moment of about 1.8×10^{20} Nm, consistent with teleseismic estimates, is found. The earthquake consisted of two main, interconnected, zones of slip located 20 and 40 km WNE of the hypocenter. Over the 15 s rupture duration the average rupture velocity was 3 km/s. The timing of the rupture is nevertheless poorly constrained due to the source depth and the problem of trade off between slip, rise time and rupture velocity in the model formulation. The early, larger aftershocks, all normal-faulting events, were shallower (depths between 32 and 38 km) and closer to the coast than the main slip zone of the mainshock. This observation along with the rupture history of the mainshock, should give insights about the state of stress of the subducting Cocos plate [*Gardi et al.,* 2000].

The recurrence period of large thrust earthquakes in this segment of the plate boundary is about 50 years [*Singh et al.,* 1981]. Since the last such event in this region occurred in 1978 (Mw=7.7), the 1999 intraslab earthquake took place roughly in the middle of the earthquake cycle. Were these two events related? The kinematic description of the source presented in this paper is a first step to study the possible stress interaction between these two events.

Acknowledgments. We are grateful to T. Mikumo for fruitful discussions. We thank M. Cocco and an anonymous reviewer for helpful comments. We thank V. Kostroglodov for his help in the preparation of the figures and M. Kikuchi for providing us with the teleseismic source-time function prior to publication. The research was partly supported by CONACYT (México) projects J32308-T and G25842-T, and DGAPA (UNAM) project IN109598.

References

Cocco, M., J.F. Pacheco, S.K. Singh, and F. Courboulex, The Zihuatanejo, Mexico earthquake of December 10, 1994 (M = 6.6): source characteristics and tectonic implications, *Geophys. J. Int., 131,* 135-145, 1997.

Cotton, F., and M. Campillo, Inversion of strong ground motion in the frequency domain : application to the 1992 Landers, California earthquake, *J. Geophys. Res., 100,* 3961-3975, 1995.

Gardi, A., M. Cocco, A. Negredo, R. Sabadini, and S.K. Singh, Dynamic Modeling of the subduction zone of Central Mexico. *Geophys. J. Int.,* Accepted, 2000.

Hernandez, B., F. Cotton, and M. Campillo, Contribution of radar interferometry to a two step inversion of the kinematic process of the 1992 Landers earthquake., *J. Geophys. Res., 104,* 13083-13099, 1999.

Mikumo, T., M.A. Santoyo, and S.K. Singh, Dynamic rupture and stress change in a normal faulting earthquake in the subducting Cocos plate, *Geophys. J. Int., 140,* 611-620, 2000.

Mikumo, T., S.K. Singh, and M.A. Santoyo, A possible stress interaction between large thrust and normal-faulting earthquakes in the Mexican subduction zone, *Bull. Seismol. Soc. Am., 89,* 1418-1427, 1999.

Singh, S.K., M. Ordaz, L. Alcantara, N. Shapiro, V. Kostoglodov, J.F. Pacheco, S. Alcocer, C. Gutierrez, R. Quaas, T. Mikumo, and E. Ovando, The Oaxaca earthquake of September 30, 1999 (M_W=7.5) : A normal-faulting event in the subducted Cocos plate, *Seism. Res. Lett., 71,* 67-78, 2000.

Singh, S.K., M. Ordaz, J.F. Pacheco, R. Quaas, L. Alcantara, S. Alcocer, C. Gutierez, R. Meli, and E. Ovando, A preliminary report on the Tehuacan, Mexico earthquake of June 15, 1999 (M_W=7.0), *Seism. Res. Lett., 70,* 489-504, 1999.

Singh, S.K., G. Suárez, and T. Domínguez, The great Oaxaca earthquake of 15 January 1931: lithosphere normal-faulting in the subducted Cocos plate, *Nature, 317,* 56-58, 1985.

Singh, S.K., J. Havskov, and L. Astiz, Seismic gaps and recurrence periods of large earthquakes along the Mexican subduction zone: a reexamination, *Bull. Seism. Soc. Am., 71,* 827-843, 1981.

Singh, S.K., J. Havskov, K. McNally, L. Ponce, T. Hearn, and M. Vassiliou, The Oaxaca, Mexico earthquake of 29 November 1978: a preliminary report on aftershocks, *Science, 207,* 1211-1213, 1980.

Tarantola, A., and B. Valette, Generalized nonlinear inverse problem solved using the least squares criterion, *Rev. Geophys. Space Phys., 20,* 219-232, 1982.

B. Hernandez and F. Cotton, IPSN, 60-68 Avenue du Général Leclerc, B.P. 6, 92265 Fontenay-aux-Roses Cedex, France. (e-mail: bhernand@chez.com)

N. M. Shapiro, S. K. Singh, J. F. Pacheco, A. Iglesias, V. Cruz and J. M. Gómez, Instituto de Geofísica, UNAM, CU, 04510 México, D.F.

M. Campillo and B. Hernandez, LGIT, Université Joseph Fourier, B.P. 53, 38041 Grenoble Cedex 9, France.

L. Alcántara, Instituto de Ingeniería, UNAM, CU, 04510 México, D.F.

(Received June 30, 2000; revised October 20, 2000; accepted October 26, 2000.)